Insights into tissue-specific anthocyanin accumulation in Japanese plum (*Prunus salicina* L.) fruits: A comparative study of three cultivars

Nan Xiang [a,d,1], Xiaoxiao Chang [b,1], Liuwei Qin [a], Kun Li [c], Siyun Wang [d], Xinbo Guo [a,*]

[a] *School of Food Science and Engineering, Guangdong Province Key Laboratory for Green Processing of Natural Products and Product Safety, Engineering Research Center of Starch and Vegetable Protein Processing Ministry of Education, Research Institute for Food Nutrition and Human Health, South China University of Technology, Guangzhou 510640, China*
[b] *Institute of Fruit Tree Research, Guangdong Academy of Agricultural Sciences, Key Laboratory of South Subtropical Fruit Biology and Genetic Resource Utilization, Ministry of Agriculture and Rural Affairs, Guangdong Provincial Key Laboratory of Tropical and Subtropical Fruit Tree Research, Guangzhou 510640, China*
[c] *Crop Research Institute, Key Laboratory of Crops Genetics Improvement of Guangdong Province, Guangdong Academy of Agricultural Sciences, Guangzhou 510640, China*
[d] *Department of Food, Nutrition, and Health, University of British Columbia, Vancouver, BC V6T 1Z4, Canada*

A R T I C L E   I N F O

A B S T R A C T

In the present study, three matured Japanese plum cultivars with different colored peel and flesh were selected to mine the key transcription factors regulating anthocyanin formation in tissues. Results showed that *PsMYB10* was correlated with structural genes *C4H*, *F3H*, and *ANS*. *PsMYB6* could positively regulate *C4H* (r = 0.732) and accumulated anthocyanins in Sanhua plum's flesh. Sanhua plum has the highest phenolic and anthocyanin contents (10.24 ± 0.37 gallic acid equivalent mg g^{-1} dry weight (DW) and 68.95 ± 1.03 μg g^{-1} DW), resulting itself superior biological activity as 367.1 ± 42.9 Trolox equivalent mg g^{-1} DW in oxygen radical absorbance capacity value and 72.79 ± 4.34 quercetin equivalent mg g^{-1} DW in cellular antioxidant activity value. The present work provides new insights into the regulatory mechanism of tissue-specific anthocyanin biosynthesis, confirming the pivotal role of anthocyanins in the biological activity of plums, providing essential support for the development of horticultural products enriched with anthocyanins.

1. Introduction

Prunus is a genus with high biodiversity in the form of trees and shrubs, including the fruits of plum, cherry, peach, nectarine, apricot and almond (Halász et al., 2021). The attractive and high economic value fruits of different species belonging to the genus have been extensively studied in recent years, especially in terms of their effects on human health (Abanoz & Okcu, 2022). With unique flavor and taste, Japanese plum fruit (*Prunus salicina* L.) is considered as a commercially important plum cultivar worldwide (Topp et al., 2012). Their consumption is associated with numerous health benefits, such as anti-inflammatory and anti-diabetic effects (Igwe & Charlton, 2016; Yu et al., 2021).The rich phenolic compounds in Japanese plum fruits increase their ability to scavenge free radicals and contribute to their high antioxidant capacity as well as biological activity. Therefore, research interests focus mainly on the high levels of phenolic compounds in plums, particularly a subclass of flavonoids known as anthocyanins (Igwe & Charlton, 2016).

Anthocyanins are water-soluble plant pigments that belong to the subgroup of flavonoids. They are derived from polyhydroxy and polymethoxy 2-phenylbenzopyrylium, and consist of a combination of a core anthocyanidin and glycosidic moieties (Smeriglio et al., 2016). Anthocyanin glycosides are known to be widespread in edible foods and have protective properties regarding chronic diseases in human (Smeriglio et al., 2016). Anthocyanins color in relation to matrix pH and confer ample pigments to plant tissues (Smeriglio et al., 2016). They are important phytochemicals in plum fruits (*Prunus salicina* L.) with concentrations reported ranging from 1.5 to 266.2 mg·100 g^{-1} fresh weight in 45 genotypes (Vizzotto et al., 2007). Given the abundance of anthocyanins in plum fruits, understanding the regulatory mechanism is essential for nutritional biofortification, and evaluating the biological activity of plums can provide insights into their health-promoting effects.

Using transcriptomic analysis, Fang et al. (2016) investigated thirteen important structural genes involved in anthocyanin biosynthesis during the development of 'Furongli' plum. In addition, the biosynthesis of anthocyanins in plum fruits (*Prunus salicina* L.) has been well-elucidated, with cinnamic acid being the precursor and involving in genes that encode enzymes cinnamate-4-hydroxylase (C4H), chalcone synthase (CHS), chalcone isomerase (CHI), flavanone 3-hydroxylase (F3H), dihydroflavonol 4-reductase (DFR), anthocyanidin synthase (ANS), anthocyanidin reductase (ANR) and leucoanthocyanidin reductase (LAR) (González et al., 2016; Li et al., 2019). The previous research on Sanhua plum (*Prunus salicina* L.) noted an increase in anthocyanin content during fruit development, together with the upregulation of structural genes (Li et al., 2019). Aside from that, the regulation of anthocyanin biosynthesis involves a complex network of genes and pathways, with a major mechanism being the transcriptional coordination of structural genes encoding biosynthetic enzymes. In detail, a number of transcription factor families, including MYB, bHLH, LBD, and NAC, are known to play important roles in regulating anthocyanin biosynthesis (Chaves-Silva et al., 2018). By applying appropriate temperature and light to "Akihime" plums, *PsMYB10.1* was found to be a positive regulator of anthocyanins accumulation in peel tissue (Fang et al., 2021a), while *PSMYB10.2* could activate *PsUFGT* and *PsGST* in the anthocyanin biosynthetic pathway in Sanyueli plum's flesh (Fang et al., 2021b). The transcriptomic results of 'Furongli' Plum reported three transcription factors included homologs of *Arabidopsis* transcription factors that were implicated in regulating anthocyanin biosynthesis, such as MYB, bHLH, and NAC (Fang et al., 2016). However, studies at the transcriptional level mainly concentrated on the development, stress response, and tissue specificity of a single plum fruit cultivar, and did not focus on the discrepancy of anthocyanins accumulation among cultivars. Although the significant differences of anthocyanin accumulation among thirteen Japanese plum cultivars were discussed to be associated with changes in some metabolites, such as organic acids, total phenolics and carotenoids (Julian Cuevas et al., 2015), the reason has not been fully explained. It is therefore desirable to identify the regulatory mechanism of anthocyanin biosynthesis that differs among plum cultivars with different colored tissues.

In our previous study, both the anthocyanin profiles and antioxidant activity of Sanhua plum during both ripening period and postharvest storage have been elucidated (Chang et al., 2019; Li et al., 2019). However, as a plum cultivar with red coloration in both peel and flesh, the regulation of anthocyanins in Sanhua plum has not been studied yet, and how this is related to fruit quality is still waiting for investigation. The present work hypothesized that there could be tissue specificity in the regulation of transcription factors on anthocyanin in plum fruits, and anthocyanin with its biological activity could contribute to plum fruits quality. Therefore, in this study, three Japanese plum fruit cultivars (*Prunus salicina* L.) were chosen for analysis: the Nai plum, which has yellow flesh and peel, the Red-leaf plum, which has yellow flesh and red peel, and the Sanhua plum, which has red flesh and peel. Transcriptomic analysis was combined with the determination of phytochemical compounds and biological activities in this study, to analyze the key transcription factors in regulating anthocyanin biosynthesis in plum tissues, which may lay the groundwork for improving the nutritional value and health benefits of plums.

2. Methods and materials

2.1. Sample collection

The trees of the three cultivars, Nai plum, Red-leaf plum, and Sanhua plum (*Prunus salicina* L.) were grown under the same conditions in the Agriculture Demonstration Base located in Fengkai County (Zhaoqing, Guangdong Province, China). Around 120 days after the full-blooming stage of each cultivar, the matured plum fruits without insects and damage were collected from plum trees, which had similar tree ages (over ten years) and growth patterns. Each biological replicate consisted of over thirty plums collected from more than one plum trees. The peel and flesh tissues of plums were separated from the whole fruits for experimental use (Fig. S1). The fresh samples were frozen by liquid nitrogen (Shengying Chemical, Guangzhou, China) and kept at −80 °C for transcriptomic analysis. Other samples were dried by vacuum freeze-drying treatment and stored at −80 °C for physiochemical analysis. Samples were labeled as NP (Nai plum peel), NF (Nai plum flesh), NW (Nai plum whole), RP (Red-leaf plum peel), RF (Red-leaf plum flesh), RW (Red-leaf plum whole), SP (Sanhua plum peel), SF (Sanhua plum flesh) and, SW (Sanhua plum whole) according to the cultivar and tissue.

2.2. Transcriptomic analysis

Three different cultivars of plums were sent to BGI (Shenzhen, China) for RNA extraction and RNA-seq from fresh whole plums and tissues. Each tissue of plums was sent with three biological replicates. Following RNA-seq, data were filtered by trimmomatic, and a total of 136 Gb of clean reads were generated. The raw data that support the findings of this study have been deposited into CNGB Sequence Archive (CNSA) of China National GeneBank DataBase (CNGBdb) with accession number CNP0004195. The clean reads from each sample were mapped to the reference genome *Prunus salicina* Sanyueli Genome v2.0 in GDR database (Jung et al., 2019), with 85–93% alignment via HISAT2. The gene expression levels in samples were shown as FPKM values in Table S1. Ballgown was used to screen for different expression genes (DEGs) in different cultivars and tissues (fold change (FC) > 2, FDR < 0.05).

2.3. Determination of saccharides and organic acids

Saccharides and organic acids were extracted and determined by a gas chromatography flame ionization detection (GC-FID) method with improvements (Liu et al., 2010). D-xylose (Yuanye Bio-Technology Co., Ltd, Shanghai, China) was chosen as the internal standard for calculating saccharides contents, while succinic acid (Yuanye Bio-Technology Co., Ltd, Shanghai, China) was used to quantify acids. The Agilent 6890 N network GC system (Aglient Technologies, Palo Alto, CA, USA) with a DB-1 chromatographic column (Aglient Technologies, Palo Alto, CA, USA) and an Agilent 7683 autosampler (Aglient Technologies, Palo Alto, CA, USA) were used. Nitrogen flow rate was 1.4 mL/min, and the sample size was 1 μL. The column temperature program was set as follows: 150 °C for 0–2 min, 150–210 °C at a rate of 6 °C/min, 210–275 °C at a rate of 40 °C/min, and 275 °C for 10 min. The values were presented as mean ± SD mg g^{-1} dry weight (DW) (n = 3).

2.4. Total phenolics extraction and determination

The total phenolics were extracted according to a reported method (Qin et al., 2022). Methanol/acetic acid (5:1, v/v) (ANPEL Laboratory Technologies Inc., Shanghai, China) was used as extractant for an

overnight extraction of 20 g powder in 4 °C. After centrifuging at 12,000 rpm for 2 min, the supernatant was collected and evaporated at 45 °C. Extracts were redissolved in methanol and stored in −20 °C until use. Total phenolics was measured by Folin-Ciocalteu method (Li et al., 2019) and data were expressed by gallic acid (Aladdin Industrial Corporation, Shanghai, China) equivalent as GAE mg g^{-1} DW (n = 3).

2.5. Anthocyanins determination

Anthocyanin components were analyzed by high-performance liquid chromatography (HPLC) method as previously reported (Qin et al., 2022). Plum extracts were used for detection with a 30 μL injection volume. A photodiode array detector (Waters, LC 2998, Milford, MA, USA) was used and equipped with a C18 column (Waters, 250 × 4.6 mm, 5 μm). 0.1% Trifluoroacetic acid/distilled water (Sigma-Aldrich, St. Louis, USA) and acetonitrile (ANPEL Laboratory Technologies Inc., Shanghai, China) were used separately as the two mobile phases. The analysis was performed by gradient elution program at 520 nm with 1 mL min^{-1} flow rate according to the previous study (Qin et al., 2022). Standards cyanidin chloride and pelargonidin chloride were purchased from Sigma-Aldrich (St. Louis, USA) and the results were calculated using the standard curve method and presented as μg g^{-1} DW (n = 3).

2.6. The analysis of antioxidant capacity

The total antioxidant evaluation was conducted by oxygen radical absorbance capacity (ORAC) assay according to the previous study (Ou et al., 2001). Plum extracts were diluted by phosphate buffer to the appropriate concentration, and then were mixed with fluorescein in 96-well plate. Then, the mixture was incubated at 37 °C for 20 min before adding the 2,2′-azobis(2-amidinopropane) dihydrochloride (Sigma-Aldrich, St. Louis, USA). The fluorescence intensity was measured at excitation of 485 nm and emission of 535 nm by FilterMax F5 Multi-Mode Microplate Reader (Molecular Devices, Sunnyvale, CA, USA). Trolox (Sigma-Aldrich, St. Louis, USA) was used as standard and results were expressed by Trolox equivalent as TE μmol g^{-1} DW.

The cellular antioxidant activity was determined by cellular antioxidant activity (CAA) assay (Wolfe & Liu, 2007). HepG2 cell lines were used as cell model for analysis and quercetin (Aladdin Industrial Corporation, Shanghai, China) was used as the standard. Both PBS (phosphate buffered saline) wash and PBS no wash treatments were used in order to evaluate the uptake of cells towards active substance. Briefly, HepG2 cells were plated in a 96-well black plate with appropriate density and incubated at 37 °C for 24 h. Then, plum extracts that diluted to specific concentration or controls were dissolved in treatment medium with 2,7-dichlorodihydrofluorescein deacetate (Sigma-Aldrich, St. Louis, USA) and added. After incubating for 1 h, cells were washed or not washed with PBS. 2,2′-azobis(2-amidinopropane) dihydrochloride (Sigma-Aldrich, St. Louis, USA) was then added and the plate was read in FilterMax F5 Multi-Mode Microplate Reader (Molecular Devices, Sunnyvale, CA, USA) at 37 °C. Results were calculated from the integrated area under the fluorescence versus time curve and were reported as mean ± SD quercetin equivalent (QE) μmol g^{-1} DW (n = 3).

2.7. Anti-proliferation activity and cytotoxicity assays

HepG2 cell lines were used to test the cytotoxicity and anti-proliferative activities. According to the published methods (Wang et al., 2017), the cells were stained with methylene blue solution (Sigma-Aldrich, St. Louis, USA) and methylene blue (BBL, Cockeysville, USA) with Hanks Balanced Salt Solution (Invitrogen) in a 96-well plate, which was then incubated at 37 °C for 1 h. Cells were then washed and dried. After eluting the Methylene blue stain, the absorbance was measured at 570 nm. The cytotoxicity and anti-proliferative activities were measured and separately expressed as CC_{50} value (dose-dependent of 50% cell death, mg mL^{-1}, n = 3) and IC_{50} value (50% inhibitory concentrations,

mg mL^{-1}, n = 3).

2.8. Weighted gene co-expression network analysis (WGCNA)

WGCNA was conducted on BMKCloud platform (available at https://www.biocloud.net, accessed on 6 May 2022) with traits. The genes in Table S1 with FPKM values >0.1 were used. Discrepancies between modules were set as 0.5 and the minimum gene number in a module was set as 30 in order to achieve the reliability of the results.

2.9. Statistical analyses

IBM SPSS 25 (IBM Corporation, Armonk, NY, USA) was used for performing Tukey analysis and Pearson correlation (p < 0.05). Venn plot were conducted on jvenn (Bardou et al., 2014) and KEGG pathway of genes were annotated according to the functional analysis data of *Prunus Salicina* genome on GDR database (Jung et al., 2019). To achieve the existed relative functions of TFs, the sequences of genes from GDR database were compared with the NCBI database via BLAST. Figures were generated from Origin 2018 (OriginLab Corporation, Northampton, MA, USA) and online websites (Bioinformatics and Metaboanalyst). The FPKM values of structural genes were normalized on Metaboanalyst using auto-scaling (mean-centered and divided by the standard deviation of each variable). All the samples were collected with three biological replicates and determined for three times. Results were exhibited as mean ± SD (n = 3).

3. Results

3.1. The analyzation of different expression genes (DEGs) of three cultivars of plums

The raw data of transcriptomic results have been deposited into CNGB Sequence Archive (CNSA) of China National GeneBank DataBase (CNGBdb) with accession number CNP0004195. The clean reads of transcriptomic results were mapping to reference genome *Prunus salicina* Sanyueli Genome v2.0 in GDR database (Jung et al., 2019). The gene expression levels in samples were shown as FPKM values in Table S1. Then, the differently expression genes (DEGs) were screened in the peel, flesh, and whole fruits of the three plum cultivars (fold change (FC) > 2, FDR < 0.05) by using T-test. A total of 1955, 45, and 1576 DEGs were detected in the compared groups of Nai plum *vs* Red-leaf plum, Nai plum *vs* Sanhua plum, and Red-leaf plum *vs* Sanhua plum in the peel, while 630, 643, and 1962 were detected in the flesh, and the quantities reduced to 7, 183 and 144 in whole fruits, respectively. From the numbers of DEGs among comparing groups, nuances were detected between the peels of Nai plum and Sanhua plum which had different colors. In addition, the transcriptomic profiles of the whole fruits of the three cultivars were similar, and Nai plum and Red-leaf plum had high proximity, shown as less DEGs. Fig. 1A depicted the Venn plot of each tissue. Taken the color of tissues into consideration, 13 DEGs from the overlapping of Nai plum *vs* Red-leaf plum and Nai plum *vs* Sanhua plum groups might be the genes that contribute to the red color of the peel (labelled as peel DEGs). Correspondingly, 234 DEGs from the intersection of Nai plum *vs* Sanhua plum and Red-leaf plum *vs* Sanhua plum groups might be the genes that are responsible for the coloration of red pigment in flesh (labelled as flesh DEGs). In Fig. 1B, the number of DEGs from peel *vs* flesh in Nai or Red-leaf plum were depicted and the number of DEGs unique to Red-leaf plum was 505. These genes might be related to the formation of different colors in the peel and flesh in Red-leaf plum (labelled as tissue DEGs). In addition, unlike Nai and Red-leaf plums, only two DEGs were found between the peel and flesh of Sanhua plum, so Sanhua plum was excluded.

Fig. S2 includes KEGG pathway classification for all the annotated DEGs in the peel or flesh tissue to identify the differences among the three cultivars in terms of relative genes. As shown, a large amount of
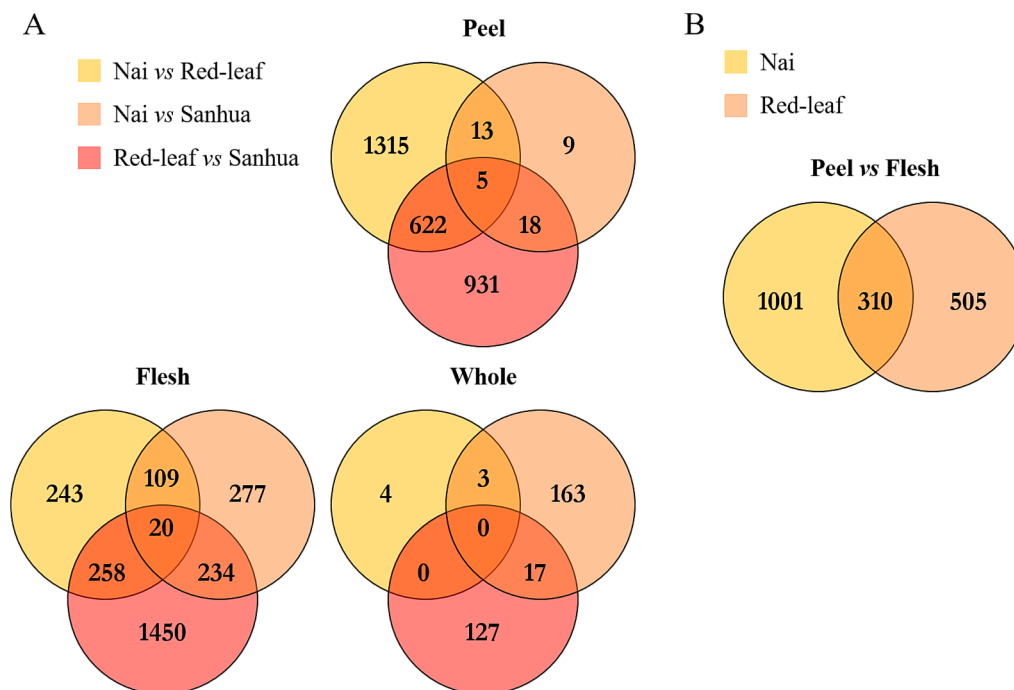
Fig. 1. The profiles of transcriptomic results. A: Venn plots of tissues in the three cultivars of plum fruits. B: Venn plot of DEGs in Nai and Red-leaf plums between peel and flesh. (For interpretation of the references to color in this figure legend, the reader is referred to the web version of this article.)

genes in both the peel and flesh tissues were classified into the metabolism category. The numbers of DEGs in both the peel and flesh tissues ranked the first in carbohydrate metabolism category, followed by amino acid metabolism and energy metabolism categories. Aside from the metabolism category, a large proportion of DEGs in both the peel and flesh tissues were also classified into signal transduction pathway category.

Specific overlapping DEGs, including the peel, flesh, and tissue DEGs mentioned above, were gathered for TF prediction on BMKCloud and results were shown in Table S2. As shown, three TFs, including the predicted *bHLH112* and *MYB10*, were identified in the flesh group. In addition, seven TFs were annotated into several TF families involving the bHLH, C2H2, HB, HSF and MYB families, which may play important roles in pigment synthesis of plums.

3.2. Saccharides and organic acids contents in three cultivars of plums

A total of four saccharides and two organic acids, including fructose, glucose, sucrose, sorbitol, malic acid and quinic acid, were detected in three cultivars of plums (Table 1). As shown, glucose was the most

Table 1
The saccharides and organic acids content in tissues of three cultivars of plum (mg g^{-1} DW, n = 3).

Cultivar	Position	Glucose	Fructose	Sorbitol	Sucrose	Malic acid	Quinic acid	Total Saccharides [2]	Total Organic Acids [3]	Ratio (S/A [4])
Nai Plum	Peel	204.0 ± 6.1c [1]	159.5 ± 3.8bc	86.24 ± 2.54c	14.08 ± 0.59de	61.69 ± 2.86bc	20.27 ± 1.00b	463.9 ± 12.9bc	81.95 ± 3.79c	5.661
	Flesh	226.7 ± 24.9bc	183.1 ± 6.7a	103.9 ± 10.1bc	25.60 ± 2.02 cd	53.43 ± 0.44cde	5.298 ± 0.231d	539.2 ± 32.4a	58.73 ± 0.44de	9.181
	Whole	231.8 ± 11.9bc	175.3 ± 5.5ab	117.4 ± 6.7b	34.28 ± 3.00c	48.40 ± 1.27e	8.666 ± 0.350c	558.8 ± 24.6a	57.07 ± 1.49e	9.791
Red-leaf Plum	Peel	240.8 ± 1.9b	95.21 ± 2.55e	85.84 ± 1.16c	ND	80.70 ± 0.70a	30.02 ± 0.51a	421.9 ± 5.2c	110.7 ± 1.0a	3.811
	Flesh	295.6 ± 18.3a	160.4 ± 9.3bc	104.4 ± 7.5bc	2.200 ± 0.055e	77.23 ± 5.52a	19.33 ± 1.66b	562.6 ± 35.0a	96.56 ± 7.00b	5.826
	Whole	285.1 ± 1.6a	150.4 ± 2.4c	103.4 ± 0.3bc	2.400 ± 0.238e	84.84 ± 2.35a	21.89 ± 1.73b	541.3 ± 3.0a	106.7 ± 2.1a	5.073
Sanhua Plum	Peel	200.1 ± 11.6c	168.5 ± 6.2ab	62.89 ± 3.42d	25.83 ± 0.10 cd	53.01 ± 2.46de	9.317 ± 0.842c	457.3 ± 21.3bc	62.32 ± 3.30de	7.338
	Flesh	116.5 ± 4.9d	92.35 ± 5.13e	151.4 ± 7.0a	139.4 ± 7.5a	59.89 ± 3.65bcd	5.545 ± 0.227d	499.6 ± 20.6ab	65.43 ± 3.82de	7.636
	Whole	137.6 ± 9.2d	113.9 ± 4.7d	146.6 ± 16.3a	104.6 ± 11.8b	61.84 ± 3.26b	5.848 ± 0.193d	502.7 ± 35.3ab	67.69 ± 3.45d	7.427

[1] Different letter in each column stands for significant differences (p < 0.05).
[2] Total Saccharides content = the sum of glucose, fructose, sorbitol and sucrose contents.
[3] Total Organic Acid content = the sum of malic acid and quinic acid contents.
[4] S/A: Saccharides/acids.

abundant saccharides in samples, followed by fructose and sorbitol. The glucose content in the flesh of Red-leaf plum was the highest (295.6 ± 18.3 mg g^{-1} DW) among the fleshes of the three cultivars, while the flesh of Nai plum had the most abundant fructose (183.1 ± 6.7 mg g^{-1} DW), and the contents of sorbitol and sucrose in the flesh of Sanhua plum was the highest (151.4 ± 7.0 and 139.4 ± 7.5 mg g^{-1} DW, separately). In particular, the contents of glucose and fructose in the peel of Sanhua plum were almost twice that of the flesh sample, while the contents of sorbitol and sucrose in the flesh of Sanhua plum were more than twice that of the peel sample. Besides, the sucrose content of Red-leaf plum was the lowest among all plums, only 2.400 ± 0.238 mg g^{-1} DW was detected in the whole fruit. Viewing from organic acids, malic acid was more abundant than quinic acid in plums, occupying 72–92% of the total. Red-leaf plum contained the highest total organic acid content in every tissue among the three cultivars, especially in the peel, the content was as high as 110.7 ± 1.0 mg g^{-1} DW. Correspondingly, the total saccharides content of the peel of Red-leaf plum was the lowest. When it comes to the S/A ratio (saccharides/acids), the ratios of Nai plum tissues were uniformly lower than that of the corresponding tissues of Red-leaf plum. Besides, the S/A values of the peels in the two cultivars were significantly lower than that of the fleshes or the whole fruits. Differently, the peel, flesh, and whole fruits of Sanhua plum all showed similar ratios around 7.

3.3. Anthocyanin profiles and biosynthesis in three cultivars of plums

The total phenolic contents of the three plum cultivars were shown in Fig. 2A. Compared with the flesh tissue, the total phenolic contents in the peel of the three plum cultivars were higher, and the content in the peel of Sanhua plum reached 25.12 ± 0.41 mg gallic acid equivalent (GAE) g^{-1} DW, which was about 4.02 times that in the Red-leaf plum's peel. In particular, the contents in the peel tissues of Sanhua and Nai plums were 3.18 and 3.23 times that of the flesh tissues, respectively. In terms of cultivars, the total phenolic content of Sanhua plum was the highest as 10.24 ± 0.37 mg GAE g^{-1} DW, which was 2.38 times the lowest total phenolics content in Red-leaf plum, while Nai plum ranked the second.

Viewing from Fig. 2B, two components of anthocyanins were identified, including pelargonin and cyanidin. Occupying 86–96% of the total anthocyanins in plums, cyanidin stood out as the most common anthocyanin. Comparing different tissues, it was found that the anthocyanin content in the peel of plum was more abundant, and the peel of Sanhua plum contained 151.6 ± 4.5 μg g^{-1} DW of cyanidin and 10.26 ± 0.51 μg g^{-1} DW of pelargonin, respectively. Notably, no anthocyanin components were found in non-red tissues, such as the Nai plum and the flesh of the Red-leaf plum.

Structural genes involved in anthocyanin biosynthesis and differentially expressed in specific tissues of the three plum cultivars were depicted in Fig. 3 with their standardized FPKM values (original data in Table S3). In the biosynthesis pathway of pelargonidin and cyanidin, *F3H* and *ANS* genes were upregulated in the peel of Red-leaf and Sanhua plums compared to Nai plum. Sanhua plum was the only cultivar that highly expressed *PAL*, *C4H*, *CHS*, *CHI*, *F3H*, and *ANS* genes in its flesh. In addition, the three *HCT* genes were noticeably upregulated in Nai plum as compared to both Red-leaf and Sanhua plums, while *F3'H* was significantly upregulated in Sanhua plum in all tissues. In the consumption pathway of the identified anthocyanins, one *BZ1* gene in the peel was only downregulated in Nai plum, whereas the other two *BZ1* genes were highly expressed in the flesh of Sanhua plum, instead of Nai and Red-leaf plums. Generally, the findings of the differentially expressed genes in the anthocyanin biosynthesis pathway could provide evidence for pigment accumulation in the peel and flesh tissues of plums.

3.4. Antioxidant, anti-proliferative and cytotoxicity activities of three cultivars of plums

The evaluations of total and cellular antioxidant activities were separately presented by oxygen radical absorbance capacity (ORAC) and cellular antioxidant activity (CAA) values (Table 2). Consistently, the ORAC values of the peel in Nai, Red-leaf, and Sanhua plums were separately 4.5, 2.1, and 3.9 times that in the flesh. Besides, the ORAC values of Sanhua plum ranked the first among the three cultivars, as 1147 ± 47, 290.4 ± 28.3, and 367.1 ± 42.9 TE μmol g^{-1} DW in the peel, flesh and whole fruits, respectively, followed by Nai plum.

In CAA method, both measurements with phosphate buffered saline (PBS) wash and without PBS wash method were used. The CAA no wash values were consistently higher in the peel than in the flesh tissue in the three studied plum cultivars, while the CAA wash value exhibited diversely with the lower values were detected in the peel of the three cultivars. However, Sanhua plum was still the cultivar that had the highest CAA values as 4.297 ± 0.185, 0.716 ± 0.037, and 1.237 ± 0.075 QE mg g^{-1} DW in the peel, flesh, and whole fruits, separately. The cell uptake ratio was calculated using the PBS wash and no wash values, and the results are shown in Table 2. Sanhua plum enjoyed the highest cell uptake rate of 50.22% among the three cultivars, which was primarily as a result of the high cell uptake rate in the peel of 72.79%.

The results of anti-proliferative activity and cytotoxicity activity of the samples were shown in Table 2. The IC$_{50}$ values (50% inhibitory concentrations, mg mL^{-1}) of the peels of Nai and Sanhua plums were lower than those of the fleshes, while the IC$_{50}$ values of Red-leaf plum's peel and flesh were similar. Besides, among the three cultivars, all the Red-leaf plum's tissues enjoyed the highest IC$_{50}$ value as 6.486 ± 0.237, 6.101 ± 0.340, and 8.709 ± 0.470 mg mL^{-1} DW in the peel, flesh, and
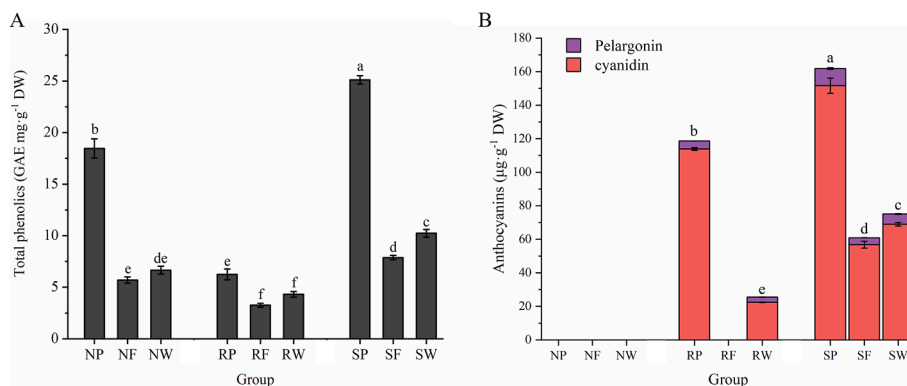
Fig. 2. A: Total phenolics content of the three cultivars of plum fruits. B: Anthocyanin profiles of the three cultivars of plum fruits. NP: Nai plum peel, NF: Nai plum flesh, NW: Nai plum whole, RP: Red-leaf plum peel, RF: Red-leaf plum flesh, RW: Red-leaf plum whole, SP: Sanhua plum peel, SF: Sanhua plum flesh, SW: Sanhua plum whole. (For interpretation of the references to color in this figure legend, the reader is referred to the web version of this article.)

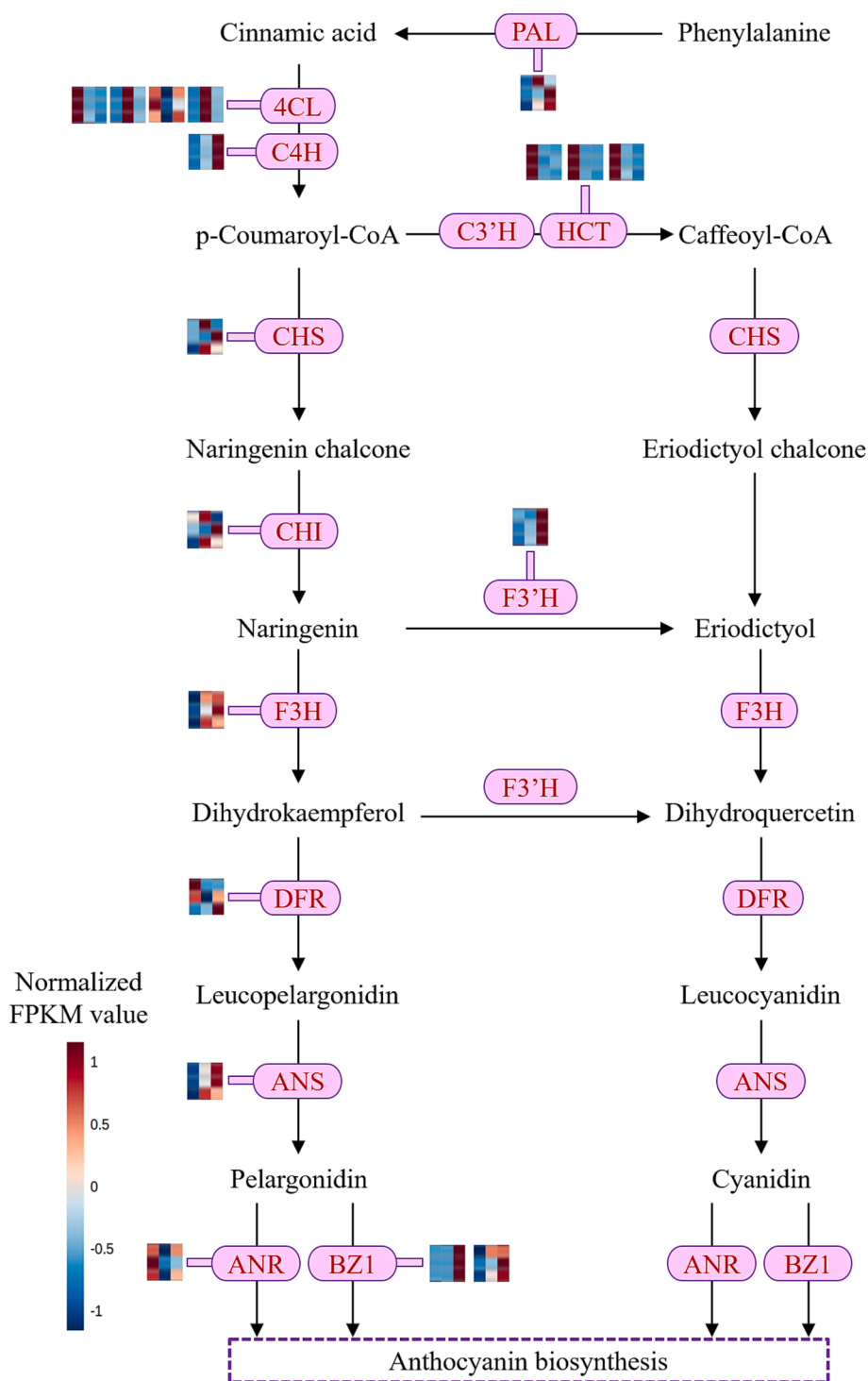**Fig. 3.** Anthocyanins biosynthesis pathway and the FPKM values of DEGs from transcriptomic results. The three rows of the heatmap separately stands for the FPKM values in peel, flesh, and whole tissues from top to the bottom, while the three columns of the heatmap separately stands for the FPKM values in Nai, Red-leaf, and Sanhua plums from left to right. PAL: phenylalanine/tyrosine ammonia-lyase, 4CL: 4-coumarate-CoA ligase, C4H: *trans*-cinnamate 4-monooxygenase, CHS: chalcone synthase, CHI: chalcone isomerase, C3′H: 5-O-(4-coumaroyl)-D-quinate 3′-monooxygenase, HCT: shikimate O-hydroxycinnamoyltransferase, F3H: naringenin 3-dioxygenase, DFR: bifunctional dihydroflavonol 4-reductase, ANS: anthocyanidin synthase, ANR: anthocyanidin reductase, BZ1: anthocyanidin 3-O-glucosyltransferase, F3′H: flavonoid 3′-monooxygenase, F3′5′H: flavonoid 3′,5′-hydroxylase. (For interpretation of the references to color in this figure legend, the reader is referred to the web version of this article.)

whole fruits, respectively. Additionally, in Nai plum, the CC_{50} value (dose-dependent of 50% cell death, mg mL^{-1}) of the peel was the lowest, only 5.725 ± 0.467 mg mL^{-1} DW. Differently, the CC_{50} values of both the peel and flesh tissues of Red-leaf and Sanhua plums showed similarities ($p < 0.05$). Moreover, each CC_{50} value of the samples consistently exceeded the corresponding IC_{50} value in the evaluation of antiproliferative activity (Table 2). Consequently, the findings illustrated that the plum extracts did not exhibit cytotoxicity at the tested concentrations of antiproliferative activity in the present study.

3.5. Weighted gene co-expression network analysis (WGCNA) results and module-trait correlation

To figure out the key TFs that potentially involved in regulating anthocyanins, WGCNA was operated on genes and traits including saccharides, organic acids, total phenolics, anthocyanins, and the evaluations of antioxidant activity. A total of 15 modules was generated including 9183 genes. The genes information in each module were listed in Table S4, and the correlation between gene modules and traits were displayed in Fig. S3. Besides, the significant positive and negative correlation values were included in Fig. 4A. As shown, the total phenolic

Table 2
Antioxidant results in *vitro* and *vivo* (n = 3).

Method	Position	Nai Plum	Red-leaf Plum	Sanhua Plum
ORAC[2] (TE μmol g^{-1} DW)	Peel	812.0 ± 78.9b[1]	192.4 ± 11.6de	1147 ± 47a
	Flesh	180.5 ± 11.0e	93.05 ± 1.92e	290.4 ± 28.3 cd
	Whole	178.3 ± 19.1e	138.1 ± 17.9e	367.1 ± 42.9c
CAA no wash[3] (QE mg g^{-1} DW)	Peel	3.613 ± 0.396b	1.040 ± 0.012d	5.909 ± 0.213a
	Flesh	0.697 ± 0.041de	0.225 ± 0.021e	2.140 ± 0.171c
	Whole	1.101 ± 0.062d	0.875 ± 0.014d	2.470 ± 0.242c
CAA wash[3] (QE mg g^{-1} DW)	Peel	1.543 ± 0.022b	0.405 ± 0.017e	4.297 ± 0.185a
	Flesh	0.253 ± 0.020ef	0.102 ± 0.014f	0.716 ± 0.037d
	Whole	0.426 ± 0.016e	0.270 ± 0.027ef	1.237 ± 0.075c
Cell uptake[4] (%)	Peel	42.98 ± 3.92bcd	38.94 ± 1.18cde	72.79 ± 4.34a
	Flesh	36.35 ± 4.32cde	45.43 ± 5.71bc	33.67 ± 4.09de
	Whole	38.81 ± 3.26cde	30.89 ± 2.62e	50.22 ± 3.16b
IC$_{50}$ Value[5] (mg mL^{-1} DW)	Peel	1.495 ± 0.034e	6.486 ± 0.237b	2.497 ± 0.052d
	Flesh	4.225 ± 0.078c	6.101 ± 0.340b	3.618 ± 0.045c
	Whole	3.869 ± 0.146c	8.709 ± 0.470a	4.157 ± 0.063c
CC$_{50}$ Value[6] (mg mL^{-1} DW)	Peel	5.725 ± 0.467e	12.64 ± 2.44bcd	11.74 ± 0.08 cd
	Flesh	11.17 ± 0.60d	14.80 ± 0.64ab	12.35 ± 0.64bcd
	Whole	17.25 ± 0.74a	14.02 ± 0.32bc	12.58 ± 0.63bcd

[1] Different letters of each index stand for significant differences ($p < 0.05$).
[2] ORAC value was used to evaluate the total antioxidant activity of samples.
[3] CAA no wash and CAA wash values were used to evaluate the cellular antioxidant activity of samples and were distinguished by whether cells were washed or not by PBS.
[4] Cell uptake = CAA wash/ CAA no wash, which was used to evaluate the uptake of cells towards active substance.
[5] IC$_{50}$ value was used to evaluate the inhibitory effect towards cells and showed the anti-proliferative activity of samples.
[6] CC$_{50}$ value was used to evaluate the cytotoxicity activity of samples.

and pelargonin contents, as well as the ORAC and CAA values, were all highly correlated with the Darkseagreen4 module (r = 0.948, 0.723, 0.934, 0.949, and 0.943, separately). In contrast, Lightcyan module was negatively correlated with phenol content and antioxidant activity in plums. A positive correlation was also found between Darkgreen module and pelargonin as correlation value r = 0.771. In addition, both glucose and quininic acid were negatively correlated with the Darkgreen and Darkviolet modules, while those modules were positively correlated to sucrose as r = 0.793 and 0.871. Modules Lightcoral and Lightcyan also possessed negative correlation values with sucrose, but they positively correlated with malic acid and quininic acid, respectively. Overall, the modules were well-separated and performed different correlation results with respect to the detected indexes in plums.
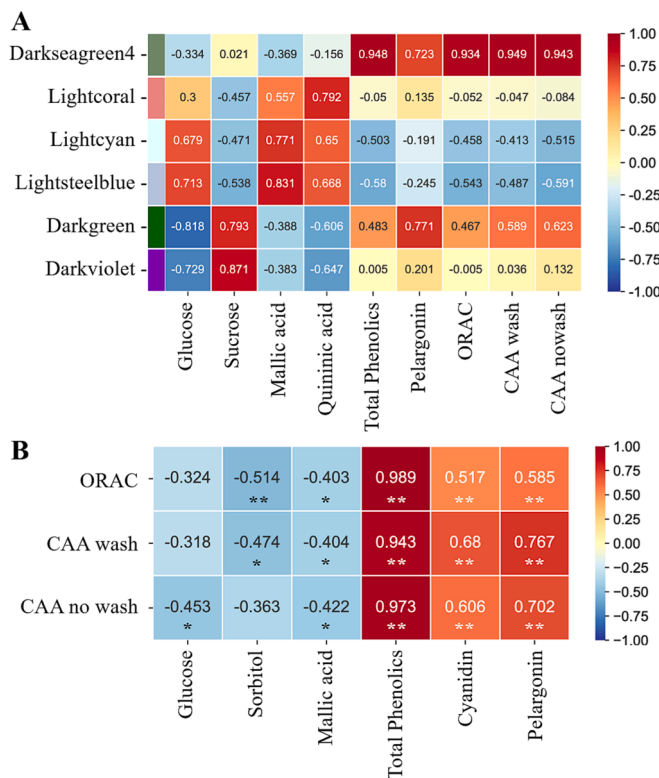
Particularly, the Darkgreen module demonstrated a strong

Fig. 4. A: The significant correlation values of modules and traits. B: The correlation values of metabolites content and antioxidant evaluative values.

correlation with pelargonin, one of the anthocyanins detected in plums. Sixteen TFs, including members of C2H2, C3H, MYB families and so on, were annotated in this module (Table S5). For the purpose of identifying the key TFs that probably control anthocyanin synthesis of plums, Pearson correlation analysis was conducted on those TFs and the potential instrumental structural genes as discussed before, the results were shown in Table S5. A total of ten TFs were supposed to be involved in the purposed process according to the correlation value (Fig. S4, p < 0.01), most of which came from C2H2, C3H, MADS and MYB families. *C4H* gene exhibited high correlation values with all the depicted TFs, while *F3H* and *ANS* were correlated to the three of them. In detail, TFs Chr1.420 (predicted *MYB6* in *Prunus mume*), Chr4.1985 (predicted *MYB51-like* in *Prunus mume*), Chr1.5810 (predicted *APL* in *Prunus mume*), Chr1.2607 (*MYB18* in *Prunus salicina*), Chr3.2093 (predicted *C3H18* in *Prunus mume*), and Chr1.548 (*MADS23* in *Prunus persica*) were included, which might be conducive to the expressions of structural genes in the present study.

4. Discussion

4.1. The formation of the desirable flavor and pigment in Sanhua plum

Soluble sugars and organic acids are the two major characteristics that contribute to fruit flavor (Jiang et al., 2019). Besides, the S/A ratio is able to denote the edible quality and maturity of plums (Li et al., 2019). In order to indicate the edible quality and maturity of the studied plums, saccharides and organic acids were determined and S/A ratio were calculated. In the flesh of stone fruits, sucrose, glucose, fructose, and the sugar alcohol sorbitol were the prominent existing soluble sugars (Walker et al., 2020). In the study operated by Singh et al. (Singh et al., 2009), four sugars were detected in Japanese plums (*Prunus salicina* Lindell), with fructose and glucose being the two most abundant. These findings were consistent with the high levels of fructose and glucose in the three *Prunus salicina* cultivars analyzed in the present

study. In addition to malic acid, which made up the majority of the total organic acids (Singh et al., 2009), quinic acid was also included in our results. Besides, when refer to the S/A ratio, the studied plum cultivars consistently had values over 3, indicating their maturity and uniformity for comparison in the present study. Despite the difference in peel and flesh colors, the S/A ratios of the peels of Nai and Red-leaf plums were obviously smaller than those in the fleshes. These results were discrepant from the findings for Sanhua plum, whose peel and flesh developed a similar red color. On the one hand, the unique high sucrose content in the flesh of Sanhua plum might contribute to its anthocyanin biosynthesis, since sucrose has previously been reported to have a specific role in inducing the upregulation of genes in the anthocyanin biosynthetic pathway (Solfanelli et al., 2006). On the other hand, malic acid was discussed being helpful for the stability of anthocyanins coloring (Munawaroh et al., 2015). Although no sucrose could be found in the peel of Red-leaf plum, it had a higher malic acid content than that in Sanhua plum, as a result, malic acid might play a potential contributing role in preserving the anthocyanins in the peel of Red-leaf plum. Although the S/A ratio of the flesh of Nai plum was high, the low S/A ratio of the peel may detract from its flavor. In light of this, the comparatively high and similar S/A ratios in both peel and flesh tissues of Sanhua plum indicated its better flavor than the other two plum cultivars. Furthermore, our previous study revealed positive correlations between total saccharides and anthocyanin production during plum ripening, suggesting a potential relationship between them (Li et al., 2019). Therefore, the abundant sucrose was contributable to Sanhua plums' anthocyanin biosynthesis, while the high content of malic acid in the peel of Red-leaf plum could in favor of the preservation of anthocyanin. Further research into the relationships between the formations of saccharides, organic acids, and anthocyanins is necessary to mine the key genes regulating anthocyanin biosynthesis in plums.

4.2. Predicted key genes in anthocyanin biosynthesis regulation

Genetic engineering has revealed the regulatory and structural genes in the anthocyanin biosynthetic pathway in a wide range of plants (Sunil & Shetty, 2022). Based on the results (Fig. 3), *F3H* and *ANS* were key genes for the anthocyanin biosynthesis in the plum peels, while *PAL*, *C4H*, *CHS*, *CHI*, *F3H*, and *ANS* genes were crucial for anthocyanin accumulation in the plum fleshes. As previously reported, the upregulations of structural genes including *4CL*, *F3H*, *F3'H*, *F3'5'H* and *UFGT* were able to accumulate flavonoids, including anthocyanins, thereby promoting the development of black skin in *Liriope spicata* fruit (Gan et al., 2022). *AhANS* has also been speculated to play a central role in anthocyanin biosynthesis in the skin of black peanuts (Huang et al., 2019). Furthermore, the upregulation of *F3'H* was supposed to introduce hydroxylation of the flavonoid B ring in order to accumulate cyanidin (Sunil & Shetty, 2022). Hence, its upregulation probably contributed to the high cyanidin content of Sanhua plum.

When it comes to the overlapping genes from the transcriptomic results (Table S2), *PsMYB10* that might regulate the anthocyanin formation in flesh tissue was included. After studying numerous cultivars of Japanese plum (*Prunus salicina*) with skin colors ranging from green and yellow to red, purple, or blue, Fiol et al. (2021) demonstrated that the PsMYB10 alleles played a significant role in plum skin coloration. The same alleles in MYB10 were also distinguished from other fruits of *Rosaceae* family, including *Prunus persica*, *Prunus dulcis*, and *Prunus avium*, as reviewed (Fiol et al., 2021). Besides, *C4H*, *F3H*, and *ANS* were correlated with *PsMYB10* (r = 0.703, 0.613, and 0.659) (Table S6, p < 0.01). *PsMYB10* was therefore predicted to interact with those structural genes to modulate anthocyanin biosynthesis in the flesh of the studied plums.

There was also a group of genes that might be involved in the discrepant color in the peel and flesh tissues of Red-leaf plums (Table S2, category tissue). *NtHDG2* was expected to play a role in enhancing flavonol content in tobacco leaves (Wang et al., 2020). Besides, AtMYB4

in *Arabidopsis* has previously been proved playing a dual role in flavonoid biosynthesis (Wang et al., 2020). Therefore, the reliability of the annotated TFs was enhanced in the present study, as they might regulate the coloration in different plum tissues by involving in anthocyanin biosynthesis.

In the TF annotation results of genes in Darkgreen module, several TFs of MYB family were correlated to the structural genes *C4H*, *F3H*, or *ANS* (Table S5). In addition, Darkgreen module was possessed of high correlation value with both sucrose and pelargonin. R2R3-MYB, bHLH TFs and WD-repeat proteins have long been considered as key regulators of anthocyanin biosynthesis in eudicots (Fiol et al., 2021). According to former research, *PpMYB6* was found to strongly activate the promoter of *PpUFGT* in peach, inducing anthocyanin biosynthesis when co-infiltrated with *PpbHLH35*, *PpbHLH51*, and *PpbHLH36-like* (Wang et al., 2022). The process was under the regulation of several saccharides, including glucose, sucrose, sorbitol, and fructose (Wang et al., 2022). The correlation analyses were operated among TFs from Darkgreen module and key structural genes (Fig. S4). The *PsMYB6* (Chr1.420: predicted *MYB6* in *Prunus mume*) found in the Darkgreen module might therefore be responsible for anthocyanin biosynthesis by upregulating *C4H* in plum's flesh, while the *bHLH36-like* (Table S2, Chr3.1348: predicted in *Prunus mume*) found in tissue DEGs might also be involved in this process. Besides, the apparent high sucrose content of Sanhua plum was supposed to synergistically activate anthocyanin biosynthesis in flesh tissue. In contrast, plenty of studies have reported that MYB6 and MYB18 are negative regulators of anthocyanin accumulation in *Rosaceae* fruits (Ding et al., 2021; Hui et al., 2019; Shi et al., 2021). In the present study, the positive correlation values did indicate the regulatory functions of those MYBs (Fig. S4, Chr1.420: predicted *MYB6* in *Prunus mume*; Chr1.2607: *MYB18* in *Prunus salicina*), whose expressions might be enhanced by the maturity of plums to prevent cells from accumulating excessive anthocyanins (Hui et al., 2019). In addition to MYB family, two TFs of C3H and MADS families (Fig. S4, Chr3.2093: predicted *C3H18* in *Prunus mume*; Chr1.548: *MADS23* in *Prunus persica*) showed their high correlation values with structural genes. Although the researches about the exact regulatory functions of *C3H18* and *MADS23* in *Prunus persica* were currently limited, studies have focused on the positive regulatory roles of TFs from both C3H and MADS families (Li et al., 2021; Wang et al., 2021).

Therefore, in addition to *HDG2* and *MYB4* that were involved in plum flesh and peel coloration, *MYB6,* under the potential influence of sucrose, were suggested to positively regulate *C4H* and lead to anthocyanin accumulation in Sanhua plum's flesh. Moreover, the extensively analyzed *MYB10* in the *Rosaceae* family might also play a significant role in anthocyanin formation by directly modulating *C4H*, *F3H*, and *ANS* genes in the flesh of plum cultivars used in this study. However, it should be noted that the results presented in this study are based on bioinformatic analysis and functional inference. While the predicted functions of the identified genes are supported by previous studies, experimental validation is needed to confirm their roles in specific biological processes. Therefore, the findings reported in this study should be considered as putative, and further investigation is required to fully understand the functions of these genes.

4.3. The prominent biological activity of Sanhua plum

Phenolics, especially their subgroup, anthocyanins, have been extensively studied due to their potential health benefits and the ability to lower the prevalence of chronic and degenerative diseases (Smeriglio et al., 2016). Among the three cultivars, Sanhua plum had the highest contents of total phenolics and anthocyanins in its peel, flesh, and whole tissues, and it consistently possessed the strongest antioxidant capacity shown by ORAC and CAA values in both *vitro* and *vivo*. The cell uptake rate also peaked at Sanhua plum, where the peel is a premium active source. Pearson correlation analysis was performed on the detected metabolites and antioxidant capacity values (p < 0.05, Fig. 4B). Total

phenolics as well as the two anthocyanins, cyanidin, and pelargonin, exhibited positive correlations with ORAC, CAA wash and CAA no wash values (p < 0.01). Additionally, glucose showed negative correlation with CAA no wash value, meanwhile, sorbitol was negatively correlated to ORAC and CAA wash values. Moreover, malic acid was negatively correlated with every value used to evaluate the antioxidant capacity of *Prunus salicina* (p < 0.05).

Notably, the total phenolic content exhibited stronger correlations with the three antioxidant evaluation values than cyanidin and pelargonin, suggesting that phenolics play a predominant role in the antioxidant activity of plum fruits. After evaluating the total phenolics, anthocyanins and carotenoid contents in 19 peach (*Prunus persica*) and 45 plum (*Prunus salicina*) genotypes, Vizzotto et al. (2007) concluded that the total phenolic content had the most consistent and highest correlation with antioxidant activity, acting decisively for the antioxidant activity of peaches and plums. In addition, the phenolic compositions also exhibited a correlation with peroxyl radical scavenging capacity value, indicating the effect of phenolics on antioxidant activity of Sanhua plum (Li et al., 2019). Moreover, the purple or red coloration in the epicarp of Mexican plum was supposed to be relative to the high antioxidant activity (Solorzano-Moran et al., 2015). As a downstream product of the phenolics synthetic pathway, the accumulation of anthocyanins implies the excitation of the pathway, hence it is possible to judge whether plums have greater antioxidant capacity by the color of the peel and flesh. Therefore, the consumption of Sanhua plum was considered to provide approaches to the largest health benefits in this study.

5. Conclusions

Summarily, in the present study, the structural genes *F3H* and *ANS* were found to be responsible for the accumulation of anthocyanins in the peels of Red-leaf and Sanhua plums, while *C4H* was identified as another gene controlling the enhancement of anthocyanins in the flesh of Sanhua plum. Combined transcriptomic data also revealed that *MYB10*, correlated to *C4H*, *F3H*, and *ANS*, was critical for anthocyanin production in plum flesh. *MYB6* played a positive role in regulating *C4H* and promoting anthocyanin accumulation in the flesh of Sanhua plum, possibly influenced by sucrose. Sanhua plum, with its red to purple colored peel and flesh, had the highest anthocyanins (68.95 ± 1.03 µg g^{-1} DW) and total phenolics contents (10.24 ± 0.37 mg GAE g^{-1} DW), resulting in the strongest antioxidant capacities and making it the most desirable cultivar among the three studied cultivars. Therefore, the present work could provide new insights into the mechanisms of anthocyanin biosynthesis in different colored plums and essential support for the development of horticultural products enriched with anthocyanins.

Declaration of Competing Interest

The authors declare that they have no known competing financial interests or personal relationships that could have appeared to influence the work reported in this paper.

Data availability

Data will be made available on request.

Acknowledgments

Authors are very thankful to the platform BMKCloud for data analyses.

Funding

This work was supported by the Science and Technology Program of

Appendix A. Supplementary data

Supplementary data to this article can be found online at https://doi.org/10.1016/j.fochms.2023.100178.

References

Abanoz, Y. Y., & Okcu, Z. (2022). Biochemical content of cherry laurel (*Prunus laurocerasus* L.) fruits with edible coatings based on caseinat, Semperfresh and lecithin. *Turkish Journal of Agriculture and Forestry, 46*(6), 908–918.

Bardou, P., Mariette, J., Escudié, F., Djemiel, C., & Klopp, C. (2014). jvenn: An interactive Venn diagram viewer. *BMC Bioinformatics, 15*(1), 293.

Chang, X., Lu, Y., Li, Q., Lin, Z., Qiu, J., Peng, C., … Guo, X. (2019). The combination of hot air and chitosan treatments on phytochemical changes during postharvest storage of 'Sanhua' Plum. *Fruits., 8*(8), 338.

Chaves-Silva, S., Santos, A. L. D., Chalfun-Júnior, A., Zhao, J., Peres, L. E. P., & Benedito, V. A. (2018). Understanding the genetic regulation of anthocyanin biosynthesis in plants – Tools for breeding purple varieties of fruits and vegetables. *Phytochemistry, 153*, 11–27.

Ding, T., Zhang, R., Zhang, H., Zhou, Z., Liu, C., Wu, M., … Yan, Z. (2021). Identification of gene co-expression networks and key genes regulating flavonoid accumulation in apple (Malus x domestica) fruit skin. *Plant Science, 304*, Article 110747.

Fang, Z.-Z., Kui, L.-W., Zhou, D.-R., Lin, Y.-J., Jiang, C.-C., Pan, S.-L., … Ye, X.-F. (2021b). Activation of PsMYB10.2 transcription causes anthocyanin accumulation in flesh of the red-fleshed mutant of 'Sanyueli' (*Prunus salicina* Lindl.). *Frontiers Plant Science, 12*, Article 680469.

Fang, Z., Lin-Wang, K., Jiang, C., Zhou, D., Lin, Y., Pan, S., … Ye, X. (2021a). Postharvest temperature and light treatments induce anthocyanin accumulation in peel of 'Akihime' plum (*Prunus salicina* Lindl.) via transcription factor PsMYB10.1. *Postharvest Biology and Technology, 179*, Article 111592.

Fang, Z.-Z., Zhou, D.-R., Ye, X.-F., Jiang, C.-C., & Pan, S.-L. (2016). Identification of Candidate Anthocyanin-Related Genes by Transcriptomic Analysis of 'Furongli' Plum (*Prunus salicina* Lindl.) during Fruit Ripening Using RNA-Seq. *Frontiers in Plant Science, 7*, 1338.

Fiol, A., García-Gómez, B. E., Jurado-Ruiz, F., Alexiou, K., Howad, W., & Aranzana, M. J. (2021b). Characterization of Japanese Plum (*Prunus salicina*) PsMYB10 alleles reveals structural variation and polymorphisms correlating with fruit skin color. *Frontiers in Plant Science, 12*, Article 655267.

Gan, S., Zheng, G., Zhu, S., Qian, J., & Liang, L. (2022). Integrative analysis of metabolome and transcriptome reveals the mechanism of color formation in Liriope spicata fruit. *Metabolites, 12*(2), 144.

González, M., Salazar, E., Cabrera, S., Olea, P., & Carrasco, B. (2016). Analysis of anthocyanin biosynthesis genes expression profiles in contrasting cultivars of Japanese plum (*Prunus salicina* L.) during fruit development. *Gene Expression Patterns, 21*(1), 54–62.

Halász, J., Molnár, A. B., Ilhan, G., Ercisli, S., & Hegedűs, A. (2021). Identification and molecular analysis of putative self-incompatibility Ribonuclease alleles in an extreme polyploid species, *Prunus laurocerasus* L. *Frontiers in Plant Science, 12*, Article 715414.

Huang, J., Xing, M., Li, Y., Cheng, F., Gu, H., Yue, C., & Zhang, Y. (2019). Comparative transcriptome analysis of the skin-specific accumulation of anthocyanins in Black Peanut (*Arachis hypogaea* L.). *Journal of Agricultural and Food Chemistry, 67*(4), 1312–1324.

Hui, Z., Kui, L.-W., Wang, F., Espley, R. V., Ren, F., Zhao, J., … Han, Y. (2019). Activator-type R2R3-MYB genes induce a repressor-type R2R3-MYB gene to balance anthocyanin and proanthocyanidin accumulation. *New Phytologist, 221*(4), 1919–1934.

Igwe, E. O., & Charlton, K. E. (2016). A systematic review on the health effects of plums (*Prunus domestica* and *Prunus salicina*). *Phytotheraphy Research, 30*(5), 701–731.

Jiang, C.-C., Fang, Z.-Z., Zhou, D.-R., Pan, S.-L., & Ye, X.-F. (2019). Changes in secondary metabolites, organic acids and soluble sugars during the development of plum fruit cv. 'Furongli' (*Prunus salicina* Lindl). *Journal of the Science of Food and Agriculture, 299*(3), 1010–1019.

Julian Cuevas, F., Pradas, I., Jose Ruiz-Moreno, M., Teodoro Arroyo, F., Felipe Perez-Romero, L., Carlos Montenegro, J., & Manuel Moreno-Rojas, J. (2015). Effect of organic and conventional management on bio-functional quality of thirteen plum cultivars (*Prunus salicina* Lindl.). *Plos One, 10*(8), Article 0136596.

Jung, S., Lee, T., Cheng, C.-H., Buble, K., Zheng, P., Yu, J., … Main, D. (2019). 15 years of GDR: New data and functionality in the Genome Database for Rosaceae. *Nucleic Acids Research, 47*(D1), D1137–D1145.

Li, J., Ma, N., An, Y., & Wang, L. (2021). FcMADS9 of fig regulates anthocyanin biosynthesis. *Scientia Horticulturae, 278*, Article 109820.

Li, Q., Chang, X.-X., Wang, H., Brennan, C. S., & Guo, X.-B. (2019). Phytochemicals accumulation in Sanhua Plum (*Prunus salicina* L.) during fruit development and their

potential use as antioxidants. *Journal of Agricultural and Food Chemistry, 67*(9), 2459–2466.

Liu, P. Z., Kallio, H., Lu, D. G., Zhou, C. S., Ou, S. Y., & Yang, B. R. (2010). Acids, sugars, and sugar alcohols in Chinese Hawthorn (*Crataegus* spp.) fruits. *Journal of Agricultural and Food Chemistry, 58*(2), 1012–1019.

Munawaroh, H., Fadillah, G., Saputri, L. N. M. Z., Hanif, Q. A., Hidayat, R., Wahyuningsih, S., & Iop. (2015). The co-pigmentation of anthocyanin isolated from mangosteen pericarp (*Garcinia Mangostana* L.) as Natural Dye for Dye-Sensitized Solar Cells (DSSC). In *10th Joint Conference on Chemistry* (Vol. 107). Solo, Indonesia.

Ou, B., Hampsch-Woodill, M., & Prior, R. L. (2001). Development and validation of an improved oxygen radical absorbance capacity assay using fluorescein as the fluorescent probe. *Journal of Agricultural and Food Chemistry, 49*(10), 4619–4626.

Qin, L., Xie, H., Xiang, N., Wang, M., Han, S., Pan, M., … Zhang, W. (2022). Dynamic changes in anthocyanin accumulation and cellular antioxidant activities in two varieties of grape berries during fruit maturation under different climates. *Molecules, 27*(2), 384.

Shi, L., Chen, X., Wang, K., Yang, M., Chen, W., Yang, Z., & Cao, S. (2021). MrMYB6 from Chinese Bayberry (*Myrica rubra*) negatively regulates anthocyanin and proanthocyanidin accumulation. *Frontiers in Plant Science, 12*, Article 685654.

Singh, S. P., Singh, Z., & Swinny, E. E. (2009). Sugars and organic acids in Japanese plums (*Prunus salicina* Lindell) as influenced by maturation, harvest date, storage temperature and period. *International Journal of Food Science and Technology, 44*(10), 1973–1982.

Smeriglio, A., Barreca, D., Bellocco, E., & Trombetta, D. (2016). Chemistry, pharmacology and health benefits of anthocyanins. *Phytotheraphy Research, 30*(8), 1265–1286.

Solfanelli, C., Poggi, A., Loreti, E., Alpi, A., & Perata, P. (2006). Sucrose-specific induction of the anthocyanin biosynthetic pathway in *Arabidopsis. Plant Physiology, 140*(2), 637–646.

Solorzano-Moran, S., Alia-Tejacal, I., Rivera-Cabrera, F., Lopez-Martinez, V., Josefina Perez-Flores, L., Pelayo-Zaldivar, C., … Ixchel Maldonado-Astudillo, Y. (2015). Quality attributes and functional compounds of Mexican plum (*Spondias purpurea* L.) fruit ecotypes. *Fruits, 70*(5), 261–270.

Sunil, L., & Shetty, N. P. (2022). Biosynthesis and regulation of anthocyanin pathway genes. *Applied Microbiology and Biotechnology, 106*(5), 1783–1798.

Topp, B. L., Russell, D. M., Neumüller, M., Dalbó, M. A., & Liu, W. (2012). Plum. In M. L. Badenes, & D. H. Byrne (Eds.), *Fruit breeding* (pp. 571–621). Boston, MA: Springer, US.

Vizzotto, M., Cisneros-Zevallos, L., Byrne, D. H., Ramming, D. W., & Okie, W. R. (2007). Large variation found in the phytochemical and antioxidant activity of peach and plum germplasm. *Journal of the American Society for Horticultural Science, 132*(3), 334–340.

Walker, R. P., Battistelli, A., Bonghi, C., Drincovich, M. F., Falchi, R., Lara, M. V., … Famiani, F. (2020). Non-structural carbohydrate metabolism in the flesh of stone fruits of the genus Prunus (*Rosaceae*) – A review. *Frontiers in Plant Science, 11*, Article 549921.

Wang, H., Guo, X., Hu, X., Li, T., Fu, X., & Liu, R. H. (2017). Comparison of phytochemical profiles, antioxidant and cellular antioxidant activities of different varieties of blueberry (*Vaccinium* spp.). *Food Chemistry, 217*, 773–781.

Wang, J., Cao, K., Wang, L., Dong, W., Zhang, X., & Liu, W. (2022). Two MYB and three bHLH family genes participate in anthocyanin accumulation in the flesh of peach fruit treated with glucose, sucrose, sorbitol, and fructose in vitro. *Plants-Basel, 11*(4), 507.

Wang, N., Shu, X., Zhang, F., Zhuang, W., Wang, T., & Wang, Z. (2021). Comparative transcriptome analysis identifies key regulatory genes involved in anthocyanin metabolism during flower development in *Lycoris radiata. Frontiers in Plant Science, 12*, Article 761862.

Wang, X.-C., Wu, J., Guan, M.-L., Zhao, C.-H., Geng, P., & Zhao, Q. (2020). *Arabidopsis* MYB4 plays dual roles in flavonoid biosynthesis. *Plant Journal, 101*(3), 637–652.

Wang, Z., Wang, S., Xiao, Y., Li, Z., Wu, M., Xie, X., … Yang, J. (2020). Functional characterization of a HD-ZIP IV transcription factor *NtHDG2* in regulating flavonols biosynthesis in *Nicotiana tabacum. Plant Physiology and Biochemistry, 146*, 259–268.

Wolfe, K. L., & Liu, R. H. (2007). Cellular Antioxidant Activity (CAA) assay for assessing antioxidants, foods, and dietary supplements. *Journal of Agricultural and Food Chemistry, 55*(22), 8896–8907.

Yu, J., Li, W., You, B., Yang, S., Xian, W., Deng, Y., … Yang, R. (2021). Phenolic profiles, bioaccessibility and antioxidant activity of plum (*Prunus Salicina* Lindl). *Food Research International, 143*, Article 110300.